Optimization of scatter estimation window setting for quantitative analysis in ^{111}In-pentetreotide single photon emission computed tomography imaging

Mizuho Hishikawa[1] **MHSc,**
Norikazu Matsutomo[1,2] **PhD,**
Tomoaki Yamamoto[1,2] **PhD**

1. Graduate School of Health Sciences, Faculty of Health Sciences, Kyorin University
2. Department of Medical Radiological Technology, Faculty of Health Sciences, Kyorin University

Keywords: Quantitative SPECT - ^{111}In-pentetreotide SPECT - Cross-calibration factor - Scatter correction - SPECT/CT

Corresponding author:
Tomoaki Yamamoto, MD, PhD
Graduate School of Health Sciences, Department of Medical Radiological Technology
Faculty of Health Sciences, Kyorin University, 5-4-1 Shimorenjaku
Mitaka, Tokyo 181-8612, Japan
Tel: +81-422-47-8000
tyamamoto@ks.kyorin-u.ac.jp

Received:
10 April 2020
Accepted revised:
15 September 2020

Abstract

Objective: The aim of this study was to validate the optimal scatter correction method and scatter estimation window setting in terms of image quality and quantitative accuracy for quantitative indium-111 (^{111}In)-pentetreotide SPECT imaging. **Materials and Methods:** We used a positron emission tomography/computed tomography (PET/CT) phantom to validate image quality and quantitative accuracy, and the SPECT images were acquired by the multi-energy window (MEW) method. The scatter estimation was performed using four kinds of energy windows (MEW1, MEW2, MEW3, and MEW4). Scatter correction was also performed using a dual-energy window (DEW) for comparison with MEW. Image quality was assessed using percent contrast (% contrast) and background variability, and quantitative accuracy was assessed using the mean standardized uptake value (SUVmean) with hot spheres. **Results:** In the quantification, all MEW settings approached the theoretical SUVmean (MEW1, 0.99±0.06; MEW2, 0.99±0.05; MEW3, 1.00±0.08; MEW4, 0.97±0.12) in contrast to DEW (0.88±0.05). The SUVmean value for scatter correction of both photopeaks for a 28 mm sphere showed the smallest difference from the theoretical value. **Conclusion:** The scatter correction method that gave optimal image quality and quantitative accuracy was MEW3 with two 20% energy windows (one over each photopeak) and four adjacent 3% scatter estimation windows (one on each side of the two photopeaks).

Hell J Nucl Med 2020; 23(3): 223-228 *Epub ahead of print: 14 December 2020* *Published online: 28 December 2020*

Introduction

Indium-111 (^{111}In)-somatostatin receptor scintigraphy (SRS) is widely used as an important imaging modality for diagnosing neuroendocrine tumour. Somatostatin receptor scintigraphy has been qualitatively assessed to grade the uptake intensity of tumours using the Krenning score [1]. Single photon emission computed tomography/computed tomography (SPECT/CT) has developed rapidly [2-8] and can evaluate tumours in the trunk of the body quantitatively [9-10]. Somatostatin receptor scintigraphy is also expected to be suitable for quantitative analysis [11]. However, although single-energy photon emitters have been investigated extensively, multi-energy photon emitters, such as ^{111}In-SRS, have not had their quantitative accuracy validated. In quantitative analysis, improving accuracy is important in order to correct for physical phenomena such as resolution recovery, attenuation and scatter [12-13]. In particular, scatter has a large effect when multi-energy photon emitters are used, such as ^{111}In at 171 and 245keV. Scattered radiation decreases image quality and quantitative accuracy; thus, these emitters require scatter correction, which is a multi-window subtraction method that can use a dual-energy window (DEW) [14] or a multi-energy window (MEW) [15-16]. A photopeak energy window and scatter estimation window are set, and SPECT count in the scatter estimation window is subtracted from that in the photopeak energy window. Quantitative accuracy depends on scatter correction [17], and optimal scatter correction is required for improving quantitative accuracy [18]. In this study, scatter correction methods were validated with respect to the effect of scatter estimation window settings on image quality and quantitative accuracy to determine the optimal scatter correction using subtraction scatter correction techniques.

Materials and Methods

SPECT/CT instrument and phantoms

All experimental data were acquired with a dual-head SPECT/CT camera (Infinia 8 Hawkeye 4, GE Healthcare, Chicago, IL, USA) equipped with a medium-energy general-purpose collimator, which had a sensitivity of 73 count/s/MBq at gallium-67 (^{67}Ga) with a 20% window and a system resolution of 11.5mm (FWHM at 10cm distance) with technetium-99m (^{99m}Tc). The quantitative accuracy was assessed using a positron emission tomography (PET)/CT phantom (Biodex Medical Systems, Shirley, NY, USA) containing a set of five spheres with inner diameters of 10, 13, 17, 22, and 28mm. The cross-calibration factor (CCF) was measured using a cylindrical phantom (diameter 20cm, height 20cm). The activity introduced into the phantom was measured using a dose calibrator (IGC-7, Aloka Co., Ltd., Tokyo, Japan), which was calibrated using a standard reference source.

SPECT acquisitions and reconstruction

To investigate the effect of energy window settings, a quantitative SPECT scan was performed on a PET/CT phantom with five hot spheres filled with ^{111}In solution (5.4kBq/mL). The sphere-to-background activity ratio was 5:1 [19]. The phantom was placed at the centre of the field of view. All projection data were obtained in step-and-shoot mode with rotation through 60 angular views. The acquisition time was set to 40s per projection. Five energy window settings were used. The pixel size was 4.42×4.42mm and the matrix was 128×128. A low-dose CT scan at 120kV and 2.5mA was performed. All SPECT images were reconstructed with ordered subset expectation maximization with resolution recovery, CT-based attenuation correction, and scatter correction. The number of subsets was 10, and the number of iterations was 5. A Butterworth filter was used as a pre-processing filter. The cut-off frequency was 0.3 cycles/cm, and the power factor was 10.

Energy window settings

Four combinations of window settings using the MEW scatter correction were evaluated (Figure 1) [15]. In addition, the DEW scatter correction method was also performed for comparison with MEW. The main photopeaks were set as ±10% energy windows centred at 171 and 245 keV in MEW1, MEW2, MEW3, and DEW. In MEW1, the sub-windows for scatter correction were set at 150keV ±1.5% and 193keV ±1.5%, one on each side of the lower photopeak (Figure 1A). The sub-windows for MEW2 were set at 215keV ±1.5% and 276keV ±1.5%, one on each side of the upper photopeak (Figure 1B). In MEW3, four sub-windows identical to those of MEW1 and MEW2 were set, one on each side of the two photopeaks (Figure 1C). In the case of MEW4, the main photopeak was set as a ±25% energy window centred at 215keV, and the sub-windows were set at 155keV ±1.5% and 276keV ±1.5% (Figure 1D). The sub-window used in the DEW was set as a ±4.5% energy window centred at 140keV (Figure 1E). The multiplication factor k, which is an index to correct scatter, was set to 1.0, which is the default value for ^{111}In according to the manufacturer.

Evaluation

Cross-calibration factor

We measured the CCF using a cylindrical phantom with a uniform distribution of ^{111}In solution (3.8kBq/mL). Because quantitative approaches use the CCF obtained from the reconstructed SPECT count, SPECT acquisition and reconstruction were the same as those used for a PET/CT phantom. The circular region of interest (ROI) was manually placed on each of the reconstructed SPECT images (Figure 2) and the

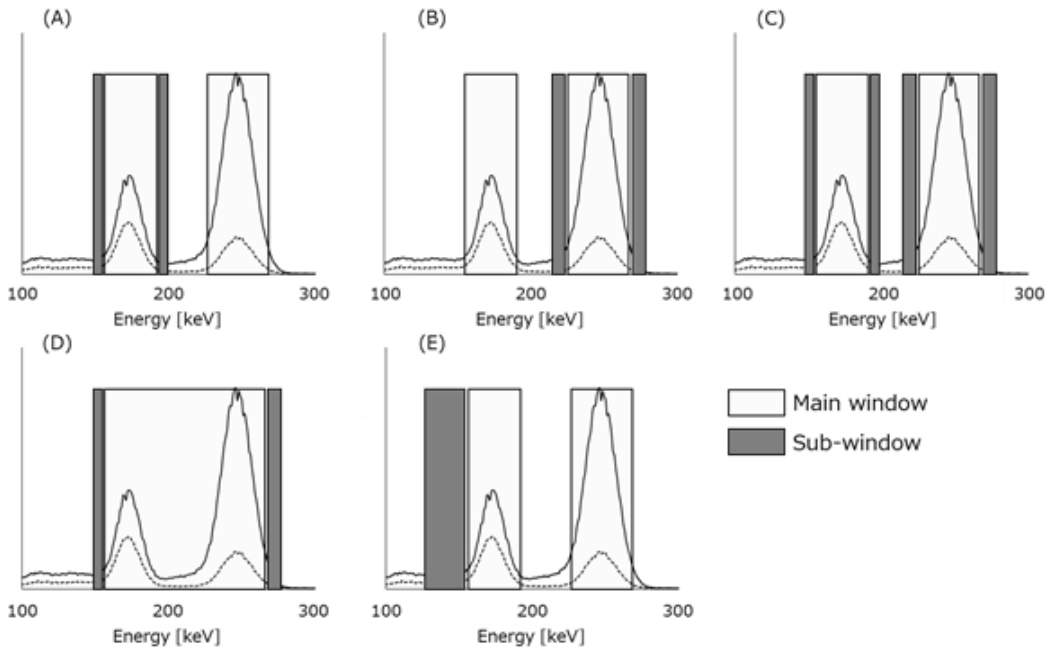

Figure 1. Energy window settings for (A) MEW1, and (B) MEW2, (C) MEW3, (D) MEW4, and (E) DEW.

CCF was calculated by:

$$\mathrm{CCF\ [Bq/cps]} = \frac{A \times T \times V_{pixel}}{M_{count} \times V_{phantom}} \quad (1)$$

where A is the decay-corrected activity at the start time of each acquisition, T is the acquisition time, Mcount is the mean count in the SPECT image ROI, Vpixel is the pixel volume, and Vphantom is the cylindrical phantom volume [20].

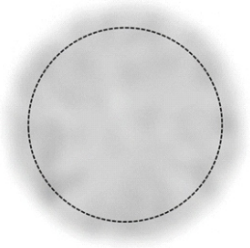

Figure 2. Schematic of the ROI setting for CCF. The ROI is enclosed in the black dashed circle.

Image quality

Image quality was assessed in terms of percent contrast (%contrast; $Q_{H,17mm}$) and background variability ($N_{B,17mm}$) [21-22]. The % contrast was set in the ROI and calculated as:

$$Q_{H,17mm} = \frac{C_{H,17\,mm}/C_{B,17\,mm} - 1}{a_H/a_B - 1} \times 100[\%] \quad (2)$$

where $C_{H,17mm}$ is mean count in the ROI for the 17mm hot sphere, $C_{B,17mm}$ is mean count calculated from 12 circular ROI of 17mm in diameter on the phantom background, a_H is the concentration in the hot sphere, and a_B is the activity concentration in the background region. The background variability in ROI was calculated as:

$$N_{B,17mm} = \frac{SD_{17mm}}{C_{B,17mm}} \times 100[\%] \quad (3)$$

$$SD_{17mm} = \sqrt{\sum_{k=1}^{K} \left(C_{B,17mm.k} - C_{B,17mm}\right)^2/(K-1)} \quad (4)$$

where SD_{17mm} is the standard deviation of the SPECT count in the background ROI, k is an index of the ROI (k=1–60), and K is the total number of ROI (K=60).

The %contrast and the background variability were calculated using a PET quality control tool for system performance (Nihon Medi-Physics Co., Ltd., Tokyo, Japan).

Quantitative analysis

The accuracy of the mean of the standardized uptake value (SUVmean) for each energy window setting was evaluated by the theoretical value (SUVmean=5.0 in a hot sphere, and SUVmean=1.0 in the background region) in a reconstructed SPECT image. We placed circular ROIs on the 28mm spheres and 12 circular ROI on the background region of the phantom at three slices (Figure 3), and evaluated them compared with the theoretical value. The value of SUVmean was calculated as:

$$\mathrm{SUV_{mean}} = \frac{M_{count} \times CCF}{T \times V_{voxel} \times A} \quad (5)$$

where V_{voxel} is the voxel volume in the reconstructed SPECT images. SUVmean was calculated using the quantitation application GI-BONE (Nihon Medi-Physics Co., Ltd.). In this study, because the system resolution was 11.5mm (FWHM at 10cm distance), we evaluated SUVmean on the 28mm hot sphere in accordance with the sampling theorem.

Statistical analysis

SUVmean obtained using each scatter window setting was compared by repeated measures single-factor ANOVA and the Tukey-Kramer test. Differences were considered statistically significant for P values of less than 0.05.

Results

Table 1 shows the % contrast and background variability obtained with different scatter estimation window settings. The % contrast obtained with the MEW was higher than that obtained with the DEW; the highest $Q_{H,17mm}$ of 44.8% was obtained with MEW3 scatter correction. The background variability obtained with MEW1, MEW3, and MEW4 was higher than that with DEW. However, the background variability obtained with MEW2 was slightly lower than that obtained with DEW.

SUVmean for each scatter estimation window for the 28 mm sphere and background settings are displayed in Table 2. SUVmean on background was 0.99±0.06 for MEW1, 0.99± 0.05 for MEW2, 1.00±0.08 for MEW3, and 0.97±0.12 for MEW4, respectively. Multi-energy windows approached the theoretical background SUVmean value (SUVmean=1.00), whereas the SUVmean value for the DEW settings was lower (0.88± 0.05). For the 28mm sphere, SUVmean obtained with MEW3 was closest to the theoretical sphere value (SUVmean= 5.00). In addition, SUVmean obtained with DEW was significantly

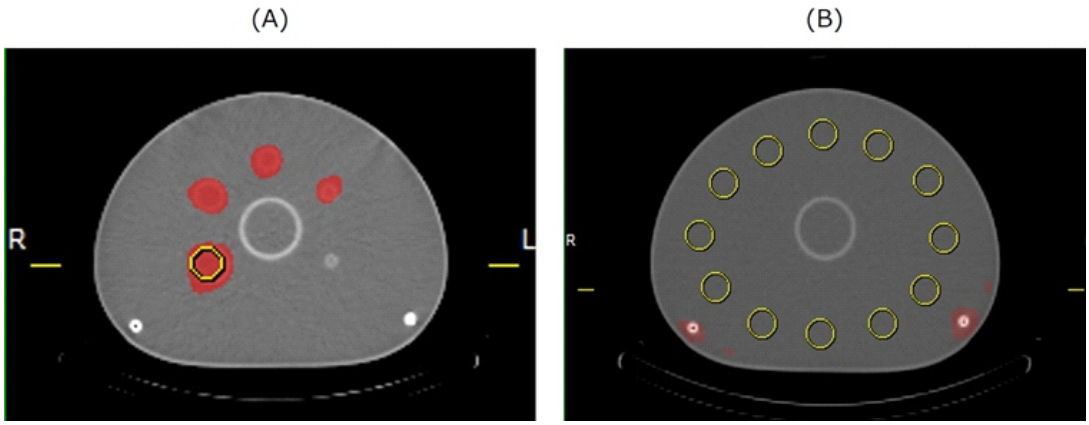

Figure 3. Schematic of the ROI setting for quantification on the 28mm hot sphere (A) and the background region (B). Each ROI is enclosed in a yellow circle. ROI were placed on the fused images (SPECT and CT).

Table 1. *Measured % contrast and background variability with different scatter estimation window settings.*

Scatter Correction	DEW	MEW			
		MEW1	MEW2	MEW3	MEW4
$Q_{H,17mm}$	42.9	43.7	43.0	44.8	39.1
$N_{B,17mm}$	10.5	12.8	9.5	15.6	29.0

DEW: dual-energy window method, MEW: multi-energy window method, *[%]*

Table 2. *SUVmean and %difference calculated using the theoretical SUVmean value for energy window settings using the MEWs and DEW scatter correction methods for the background and the 28mm hot sphere.*

Scatter Correction	SUVmean		%difference with the theoritical SUVmean value (%)	
	Background	28mm sphere	Background	28mm sphere
DEW	0.88±0.09	2.41±0.05	12.0	51.8
MEW1	0.99±0.08	2.55±0.03 *	1.0	49.0
MEW2	0.99±0.07*	2.39±0.03	1.0	52.2
MEW3	1.00±0.12	2.66±0.04* **	0.0	46.8
MEW4	0.97±0.15	2.48±0.03*	3.0	50.4

Theoretical SUVmean values
Background = 1.0,
28mm sphere = 5.0

**P<0.05 vs. DEW*
***P<0.05 vs. All MEW*

lower than that obtained with MEW1, MEW3, and MEW4. However, none of the energy window settings produced SUVmean on a 28mm sphere identical to the theoretical sphere SUVmean value.

Discussion

We validated the optimal scatter correction method and scatter estimation window settings for SRS in terms of image quality and quantitative accuracy. The MEW method was superior to the DEW method for image quality and quantitative accuracy, with higher % contrast, lower background variability, and an SUVmean closest to the theoretical value when the scatter estimation windows were set over each

^{111}In photopeak.

The image quality obtained with the DEW method was lower than that obtained with the MEW method, and SUVmean obtained with the DEW method was different from the theoretical value. The DEW scatter correction method is appropriate for a single-energy photon emitter, but not for a multi-energy photon emitter [23]. The scatter estimation window requires more than three windows for multi-energy photon emitters [15]. Furthermore, it has been reported that measurement error increased when DEW rather than MEW scatter correction is used [17]. Consistent with these previous findings, our results also indicated that the MEW scatter correction method is suitable for quantitative ^{111}In-SRS. However, multiplication factor *k* was fixed as 1.0 in our study. Factor *k* is the subtraction weighting factor for DEW, and it is common to use a value of 0.5 for ^{99m}Tc. Quantitative accuracy is affected by k [18]; thus, the effect of *k* on quantitative accuracy for ^{111}In should be measured.

The best % contrast was obtained for the MEW3 settings, in which each of the 171 and 245keV photopeaks had adjacent scatter estimation windows. Scatter estimation windows around each photopeak allowed the scattered radiation to be estimated more accurately than windows at only one of the photopeaks. Therefore, the %contrast obtained with MEW3 settings was higher. The background variability obtained with MEW3 settings was higher than those obtained with MEW1 and MEW2 settings. Background variability is a problem with the MEW method because scattered radiation is estimated and subtracted. The background variability affected the low-contrast resolution and visual image quality; thus, the MEW method requires a balance between %contrast and background variability.

In the MEW method, SUVmean for the background was close to the theoretical value regardless of the scatter estimation window (differing by 0%-3%). Acquisition and reconstruction parameters used for CCF measurement are identical to those used for imaging of subjects in quantitative SPECT. Consequently, the effect of scatter estimation setting is thought to be reflected in both CCF and SPECT images of subjects. For this reason, the MEW method showed good quantitative accuracy in SRS. This result suggests that the versatility of the CCF method is high.

SUVmean obtained with MEW3 for the 28mm sphere showed the smallest difference from the theoretical value, as with the result for % contrast. When the scatter estimation windows were set on each of the photopeaks, the % contrast increased because SUVmean was close to the theoretical value. For multi-energy photon emitters, the quantitative accuracy is reduced by downscattered component [25]. Therefore, based on our results, the MEW scatter correction method with scatter estimation windows adjacent to each side of both photopeaks is suitable for assessing SRS quantitatively.

However, our results showed underestimation in the measurement of SUVmean on hot spheres. The underestimation of the quantitative values in the structures is caused by the partial- volume effect. If the partial-volume effect at object boundaries is considered, then we could improve the spatial resolution to achieve better quantification.

The optimized scatter estimation window setting MEW with four sub-windows, one on each side of two photopeaks was shown to improve the quality and quantitative accuracy of ^{111}In SPECT images. Yamauchi et al. (2014) [26] reported that it was necessary to improve scatter correction to increase quantitative accuracy. Dewaraja et al. (2009) [27] reported that accurate quantification for image-based dosimetry in radiotherapy needs correction methods, such as resolution recovery, attenuation, and scatter correction.

There are two main limitations to this study. First, we did not evaluate clinical data; the phantom is a model corresponding to an average patient. Second, our study only used one SPECT/CT instrument, but SPECT image may differ between instruments [28], so it is important to examine different instruments. Therefore, further studies are needed to validate these results in clinical examinations using commercially available devices.

In conclusion, MEW scatter correction provided ^{111}In-pentetreotide SPECT image quality and quantitative accuracy superior to that of DEW scatter correction. The settings in which scatter estimation windows were placed on each side of the photopeak showed good results. Quantitative analysis in ^{111}In-pentetreotide SPECT imaging was achieved using MEW settings with two ±10% photopeak windows, one over each of the 171 and 245keV photopeak, and four adjacent ±1.5% scatter estimation windows, one on each side of two photopeak.

Bibliography

1. Kwekkeboom DJ, Krenning EP. Somatostatin receptor imaging. *Semin Nucl Med* 2002; 32(2): 84-91.
2. Chang LT. A method for attenuation correction in radionuclide computed tomography. *IEEE Trans Nucl Sci* 1978; NS-25: 638-43.
3. Frey EC, Tsui BMW. A new method for modeling the spatially-variant, object-dependent scatter response function in SPECT. *IEEE* 1996; 2: 1082-86.
4. Beekman FJ, Kamphuis C, Frey EC. Scatter compensation methods in 3D iterative SPECT reconstruction: a simulation study. *Phys Med Biol* 1997; 42(8): 1619-32.
5. El Fakhri G, Buvat I, Benali H et al. Relative impact of scatter, collimator response, attenuation and finite spatial resolution corrections in cardiac SPECT. *J Nucl Med* 2000; 41(8): 1400-8.
6. He B, Du Y, Song X et al. A Monte Carlo and physical phantom evaluation of quantitative In-111 SPECT. *Phys Med Biol* 2005; 50(17): 4169-85.
7. Cheng L, Hobbs RF, Segars PW et al. Improved dose-volume histogram estimates for radiopharmaceutical therapy by optimizing quantitative SPECT reconstruction parameters. *Phys Med Biol* 2013; 58(11): 3631-47.
8. Rong X, Frey EC. A collimator optimization method for quantitative imaging: application to Y-90 bremsstrahlung SPECT. *Med Phys* 2013; 40(8): 082504.
9. Zeintl J, Vija AH, Yahil A et al. Quantitative accuracy of clinical ^{99m}Tc SPECT/CT using ordered-subset expectation maximization with 3-dimensional resolution recovery, attenuation, and scatter correction. *J Nucl Med* 2010; 51(6): 921-8.
10. Beck M, Sanders JC, Ritt P et al. Longitudinal analysis of bone metabolism using SPECT/CT and ^{99m}Tc-diphosphonopropanedicarboxylic acid: comparison of visual and quantitative analysis. *EJNMMI Res* 2016; 6(1): 60.
11. Rowe SP, Vicente E, Anizan N et al. Repeatability of Radiotracer Uptake in Normal Abdominal Organs with ^{111}In-Pentetreotide Quantitative SPECT/CT. J Nucl Med 2015; 56(7): 985-8.
12. Karimi Ghodoosi E, D'Alessandria C, Li Y, et al. The effect of attenu-

ation map, scatter energy window width, and volume of interest on the calibration factor calculation in quantitative ^{177}Lu SPECT imaging: Simulation and phantom study. *Phys Med* 2018; 56: 74-80.
13. Holstensson M, Hindorf C, Ljungberg M et al. Optimization of energy-window settings for scatter correction in quantitative ^{111}In imaging: comparison of measurements and Monte Carlo simulations. *Cancer Biother Radiopharm* 2007; 22(1): 136-42.
14. Jaszczak RJ, Greer KL, Floyd CE Jr et al. Improved SPECT quantification using compensation for scattered photons. *J Nucl Med* 1984; 25(8): 893-900.
15. Ogawa K, Harata Y, Ichihara T et al. A Practical Method for Position - Dependent Compton - Scatter Correction in Single Photon Emission CT. *IEEE Trans Med Imaging* 1991; 10(3): 408-12.
16. Ichihara T, Ogawa K, Motomura N et al. Compton Scatter Compensation Using the Triple-Energy Window Method for Single- and Dual-Isotope SPECT. *J Nucl Med* 1993; 34(12): 2216-21.
17. de Nijs R, Lagerburg V, Klausen TL, Holm S. Improving quantitative dosimetry in ^{177}Lu-DOTATATE SPECT by energy window-based scatter corrections. *Nucl Med Commun* 2014; 35(5): 522-33.
18. Bailey DL, Willwson KP. Quantitative SPECT/CT: SPECT joins PET as a quantitative imaging modality. *Eur J Nucl Med Mol Imaging* 2014; 41(Suppl 1): S17-25.
19. Jönsson L, Stenvall A, Mattsson E et al. Quantitative analysis of phantom of ^{111}In and ^{68}Ga imaging of neuroendocrine. *EJNMMI Phys* 2018; 5(1): 5.
20. Matsutomo N, Matsumoto S, Yamamoto T, Sato E. Validation of a calibration method using the cross-calibration factor and system planar sensitivity in quantitative single-photon emission computed tomography imaging. *Radiol Phys Technol* 2017; 10(4): 439-45.
21. JSNMT produce guideline for FDG-PET/CT imaging 2.0. *JSNMT* 2013; 33: 377-420.
22. JSNMT produce guideline for bone SPECT imaging 1.0. *JSNMT* 2017; 37: 517-30.
23. Delpon G, Ferrer L, Lisbona A, Bardiès M. Impact of scatter and attenuation corrections for iodine-131 two-dimensional quantitative imaging in patients. *Cancer Biother Radiopharm* 2003; 18(2): 191-9.
24. Koral KF, Swailem FM, Buchbinder S et al. SPECT Dual-Energy-Window Compton Correction: Scatter Multiplier Required for Quantification. *J Nucl Med* 1990; 31(1): 90-8.
25. Motomura N, Ichihara T, Takayama T et al. Practical Compensation Method of Downscattered Component Due to High Energy Photon in ^{123}I Imaging. *Kaku igaku* 1999; 36(9): 997-1005. (Japanese)
26. Yamauchi M, Imabayashi E, Matsuda H et al. Quantitative assessment of rest and acetazolamide CBF using quantitative SPECT reconstruction and sequential administration of ^{123}I-iodoamphetamine: comparison among data acquired at three institutions. *Ann Nucl Med* 2014; 28(9): 836-50.
27. Dewaraja YK, Wilderman SJ, Koral KF et al. Use of integrated SPECT/CT imaging for tumor dosimetry in I-131 radioimmunotherapy: a pilot patient study. *Cancer Biother Radiopharm* 2009; 24(4): 417-26.
28. Onishi H, Motomura N, Fujino K et al. Quantitative performance of advanced resolution recovery strategies on SPECT images: evaluation with use of digital phantom models. *Radiol Phys Technol* 2013; 6(1): 42-53.